THE JOURNAL OF PHYSICAL CHEMISTRY C

Article

pubs.acs.org/JPCC

Electronic Properties of DNA Nucleosides Adsorbed on a Au(100) Surface

Diana Bogdan and Cristian Morari*

National Institute for Research and Development of Isotopic and Molecular Technologies, 65-103 Donath Street, 400293 Cluj-Napoca, Romania

ABSTRACT: The geometrical properties and electronic structure of single DNA nucleosides (deoxyadenosine, deoxythymidine, deoxyguanosine, deoxycytidine) adsorbed on a metallic surface of Au(100) are determined using density functional theory computations. We investigate multiple adsorption geometries and the resulting molecule−surface interaction mechanisms. For adenosine, we found negligible differences between the binding energy in the two configurations investigated by us, while for guanosine this difference reaches the maximum value among the four nucleosides (i.e., 0.38 eV). The projected density of states indicates that the physisorption is the main cause of the binding energy. Nevertheless, for the adsorbed deoxycytosine (dC), we point out the presence of the chemical interaction too. While the absolute values of the molecule−surface charge transfer are small, they are qualitatively dependent on the orientation of the nucleosides to the surface. If the DNA bases are oriented perpendicular to the surface, the electronic population of molecules decreases, while the parallel orientation of the DNA bases with respect to metal surface leads to an increase of electronic population on the molecules.

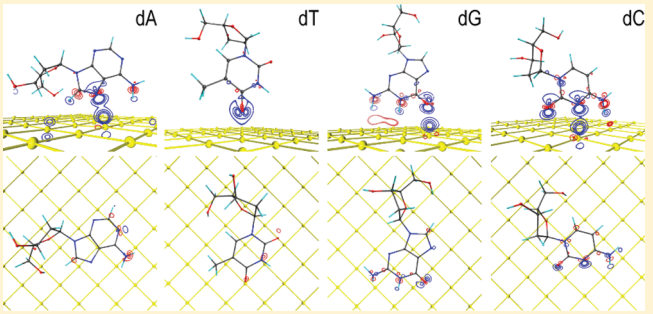

INTRODUCTION

The physical and chemical properties of molecules at surfaces play an important role in various fields, ranging from heterogeneous catalysis to nanoscale mechanics and organic optoelectronics.[1] While the properties of individual molecules can be modified in a controlled manner by chemical synthesis, their anchoring at surfaces can give rise to new functionalities, which may be used to design surfaces with specific properties.[2−5] The physical and chemical properties of such functionalized surfaces are determined by their geometric structure (e.g., orientation with respect to surface) and the electronic structure, which determines their optical, chemical, and charge transport properties. The exploitation of the self-assembly properties of oligonucleotides is widely used for such applications.

In this context, the nature of DNA−gold interactions plays an important role with many potential applications in nano- and biotechnology[6−16] (and references therein). For example, nonspecific interaction between the individual nucleotides and the gold surface favors wrapping of the DNA across surfaces (or around metal nanoparticles). On the other hand, specific bonds may favor the covalent attachment of as many DNA bases as possible with specific groups oriented to the metal surface, with the rest of the oligonucleotides directed toward the surrounding solution. Finally, entropy favors the dangling part of the oligonucleotides to adopt a random coil conformation. The understanding of the subtle interplay between these forces is crucial for the design of DNA-based nanodevices.

The DNA backbone is a polymer with an alternating sugar−phosphate sequence. The monomer units of DNA are nucleotides, consisting of a 5-carbon sugar (deoxyribose), a nitrogen-containing base attached to the sugar, and a phosphate group. Nucleosides differ from nucleotides in that they lack phosphate groups. The four different nucleosides of DNA are deoxyadenosine (dA), (deoxy)thymidine (dT), deoxyguanosine (dG), and deoxycytidine (dC), their corresponding names being associated to the types of nitrogenous bases found in DNA: adenine (A), thymine (T), guanine (G), and cytosine (C).

Recent experimental studies have shown that the DNA bases interact with Au surfaces and Au clusters in a complex and sequence-dependent manner.[17−22] The relative affinities of the homooligonucleotides to adsorb on polycrystalline Au films are ordered as A > C > G > T.[17] Mirkin and co-workers have recently shown that the heats of desorption of the nucleic acid bases from Au thin films vary within 26.3−34.9 kcal mol^{-1} and obey the following order: G > A > C > T.[18]

Adenosine and adenine have been reported to adsorb on noble metal surfaces in a planar[23−25] or nonplanar[18,20,26−29] conformation due to interactions with the surface via *N*1, *N*7, the external amino group, or the purine ring. Studies on the organic reactivity of the adenine molecule have revealed that the *N*3 and *N*9 sites are more reactive functionalities than the

Received: October 25, 2011
Revised: January 31, 2012
Published: March 10, 2012

external amino group.[30] The SERS spectra suggest that adenosine (dA) mainly binds to gold nanoparticles via the *N*7 nitrogen atom of the imidazole ring, while the *C*6−NH_2 group also participates in the coordination process. Chen et al.[19] and Giese and McNaughton[20] have also suggested that adenine binds Au via the *N*6 exocyclic amino group and the *N*7 atom. Theoretical studies show that the adsorption configurations of adenine on (110) surfaces of Cu, Ag, and Au are similar.[31] Precisely, the adenine was found to bind via the amine-N atom to the substrate, in a geometrical configuration near parallel to the surface.

Thymidine (dT) adsorption on Au(111) and Cu(110) surface studies by photoemission spectroscopy revealed that the thymine moiety is lying nearly parallel to the Au(111) surface, while on the Cu(110) surface, it adsorbs at a steep angle.[32,33] Using scanning tunneling microscopy (STM), Yang et al.[34] found that deoxyribose groups of thymidine adsorbed onto the Au(111) surface have remarkably enhanced intermolecular interaction. At low temperature, molecules form a dimer structure on the surface, while at room temperature, the thymidine molecules aggregate into well-ordered dimer islands. Finally, surface-enhanced Raman spectroscopy (SERS) study of Jang[35] shows that dT binds to the gold surfaces via the oxygen of the *C*4═O group of the pyrimidine ring. Accordingly, the nitrogen atom of an imidazole or pyrimidine ring in DNA nucleosides can be bound stronger to a gold surface than the oxygen atom of a carbonyl group.

The coordination of guanosine (dG) to the gold surface, as described by SERS spectra, is realized via the *N*1 atom and the oxygen of the *C*6═O group of the pyrimidine ring.[35] The geometrical configuration proposed indicates that the pyrimidine ring of dG adopts preferably a perpendicular position on the gold surface through the nitrogen N1 atom. Another study performed by Pergolese et al. evidenced that guanosine adsorbs on gold nanoparticles through the guanine moiety.[36] This study pointed out that the molecular sites involved in the interaction with the gold surface are the oxygen of the carbonylic group and the *N*7 atom. They argue that guanosine adsorbs on the gold substrates with a slightly tilted orientation with respect to the metal surface.

Finally, for the cytidine (dC), the SERS experiments show that the bonding to the gold surface is realized via the *N*3 nitrogen atom of the pyrimidine ring with a partial contribution from the oxygen of the *C*2═O group.[35]

The understanding of the adsorption mechanism of DNA nucleosides on Au(100) surfaces asks for a thorough investigation of the physical properties at the molecular scale. By means of the DFT models, we perform a detailed description of the geometric structure of the nucleosides adsorbed on Au(100) surfaces. The intrinsic complexity of such an investigation, stemming in the complex geometric structure of the nucleosides, is taken into account by the investigation of several possible adsorption geometries. We perform explicit investigation of two situations: the DNA bases adsorbed nearly perpendicular to the surface and the bases absorbed parallel to the surface. While both orientations are energetically stable, the second one (i.e., the DNA base adsorbed parallel to the surface) is the most stable. We investigate the projected density of states (PDOS) and molecule−surface charge transfer effects to elucidate the nucleotide−surface binding mechanisms. We analyze the atomic contributions to the HOMO orbitals of the free and adsorbed molecules. These allow us to get valuable information on the hybridization mechanism. Our results are substantiated by detailed analysis of the modification of bond lengths upon the adsorption and the molecule−surface charge transfer. While the adsorption energies indicate the physisorption as the leading adsorption mechanism, for the dC we point out major changes in the structure of frontier orbitals of the adsorbed molecule.

This article is organized as follows. We present the details of our computational approach; next, we analyze the geometrical data provided by DFT simulation. We corroborate these results with electronic structure investigations. Finally, we present an investigation of the charge transfer occurring in the four systems. We summarize our findings in the last section.

COMPUTATIONAL DETAILS

DFT is employed as the first-principles quantum mechanical method. It provides efficient and typically accurate estimates of the energies of molecule−crystal binding, molecular dissociation, surface atom rearrangements, and the overall electronic structure of a system.[37,38]

It is well-known that the DFT with a plane-wave basis set properly models electronic properties of bulk materials with Bloch-like wave functions spreading over the entire unit cell. Finite size systems, such as organic molecules, are more efficiently described by the DFT with localized basis sets. Yet, for the study of molecular adsorption, the system under consideration consists of both types of materials.

First-principles DFT calculations reported here were performed using the SIESTA method[39,40] that combines the advantages of localized basis sets with those of periodic systems. The PBE version of GGA[41] was used for electron exchange and correlation. Core electrons were replaced by norm-conserving pseudopotentials in their fully nonlocal formulation.[43] A uniform mesh with a plane-wave cutoff of 200 Ry was used for integrations in the real space.[39] We have used a standard double-ζ polarized (DZP) basis set, namely, a double (split valence) basis for each valence orbital plus polarization functions in all the atoms. The cutoff radii for the atomic orbitals of each element were obtained for an energy shift of 120 meV. This value was optimized to describe the experimental results on the geometry of DNA nucleosides. For this optimization, we use the simplex algorithm provided with the SIESTA package.[42]

Periodic boundary conditions were used to describe the infinite close-packed face-centered cubic (fcc) Au(100) surface. The spurious periodicity in the direction perpendicular to the surface is suppressed by a 21.5 Å vacuum layer between the periodic images of the systems in the *Z*-direction. The size of the cell along the *X* and *Y* axes is dictated by the requirement of isolating the base from its periodic replicas. Thus, the simulation cell contains 100 Au atoms, consisting of a four-layer 5 × 5 periodically repeated slab of the Au(100) surface and one DNA nucleoside. We use a 3 × 3 × 1 Monkorst−Pack grid for the integrals in the Brillouin zone.

Since the available experimental data suggest different adsorption configurations, we explicitly investigate two initial geometric models of the nucleosides adsorbed on the Au(100) surface. The first set of models was built according to suggestions made by Jang:[35] the DNA bases are oriented almost perpendicular with respect to the metal surface. Throughout the paper, we will call this the perpendicular orientation.

In the second set of models, a parallel orientation of the DNA base with respect to the surface was used as suggested by

Table 1. Minimum and Maximum Distance Between Nucleoisde's Atoms (Indicated in Parentheses) and the Surface (D_{min} and D_{max}), Adsorption Energy (ΔE_{ads}), and Deformation Energy (ΔE_d) for DNA Nucleosides Adsorbed on Au(100)

		dA/Au	dT/Au	dG/Au	dC/Au
perpendicular orientation	D_{min} [Å]	1.95 (H8)	2.55 (H5)	1.93 (H1)	1.83 (H4)
		2.41 (N7)	3.89 (N3)	2.95 (N1)	2.45 (N3)
		2.71 (C8)	3.17 (C4)	3.36 (C6)	2.90 (C2)
		2.52 (O4′)	1.91 (O4)	2.52 (O6)	2.17 (O2)
	D_{max} [Å]	7.31 (H2)	9.91 (H4′)	12.01 (H5′)	8.89 (H5′)
		6.00 (N3)	5.96 (N1)	6.85 (N9)	4.29 (N1)
		6.24 (C2)	8.84 (C4′)	11.02 (C5′)	8.24 (C5′)
		4.78 (O5′)	9.48 (O3′)	11.10 (O5′)	8.03 (O5′)
	ΔE_{ads} [eV]	−0.53	−0.41	−0.27	−0.46
	ΔE_d [eV]	0.06	0.00	0.07	0.07
parallel orientation	D_{min} [Å]	2.22 (H5′)	2.25 (H5′)	2.27 (H2)	2.26 (H4)
		2.64 (N1)	2.83 (N3)	2.85 (N1)	2.45 (N3)
		2.76 (C2)	2.87 (C4)	2.67 (C6)	2.61 (C2)
		2.67 (O4′)	2.62 (O4′)	2.35 (O6)	2.38 (O2)
	D_{max} [Å]	6.04 (H3′)	6.79 (H3′)	5.62 (H2)	5.79 (H3′)
		3.21 (N9)	3.25 (N1)	3.27 (N9)	3.05 (N1)
		5.01 (C3′)	4.99 (C3′)	4.92 (C2)	4.92 (C3′)
		6.11 (O3′)	5.89 (O3′)	4.53 (O3′)	5.98 (O3′)
	ΔE_{ads} [eV]	−0.53	−0.52	−0.69	−0.53
	ΔE_d [eV]	0.13	0.13	0.04	0.20

several theoretical and experimental works.[23−25,32,33] In our models, the *C5′* sugar atom was oriented toward the metal surface (i.e., allowing the furanosic oxygen and *O5′* to interact with gold atoms). Preliminary tests confirm that the binding energy is stronger in this configuration compared to the one with the *C5′* sugar atom oriented opposite to the surface, with respect to the DNA base plane. Throughout the paper, we will call this geometry the parallel orientation.

For all these models, we allow a full relaxation of the nucleosides, as well as the relaxation of the first layer of metallic surface to obtain the final geometric models. The maximum gradient accepted was set to 0.02 eV/Å.

RESULTS AND DISCUSSION

Geometry of DNA Nucleosides Adsorbed onto the Au(100) Surface. A nearly planar orientation of the nucleotides with respect to the metal surface provides the best overlap of the delocalized π-orbitals of the aromatic ring with the d-electrons of Au. Tilt orientation, on the other hand, allows the highly electronegative atoms (i.e., oxygens and nitrogens) of the DNA base to come closer to the gold atoms so that they can participate in the coordination bonding. Thus, in the cases of nucleotides adsorbed on gold surfaces, there is an interplay between two competing processes. On one hand, the π-structure of the bases' aromatic rings favors a flat orientation of the base above the Au substrate (to increase the overlap with d-orbitals). On the other hand, atoms with high electronegativity try to approach Au atoms as closely as possible to create coordination bonds.

The presence of the sugar in the molecular structure brings two new elements. First, the sugar moiety interacts directly with the gold surface (in particular, via its oxygen atoms). Second, a charge transfer occurs between the DNA base and the sugar.[44] As a consequence, the electronic charges localized over the atoms from the DNA base are slightly perturbed with respect to their values in the corresponding isolated bases.

We summarize the nucleotide−surface distances for the relaxed structures in Table 1. For the perpendicular orientation, the smallest distance to the surface is slightly less than 2 Å (with a minimum of 1.83 Å for dC). In the case of dT, the closest atom to the surface is the *O4* atom. For all the other nucleosides, hydrogen atoms are the closest atoms to the surface. For parallel orientation, we first note the value for the average distance between the π ring and the surface which is slightly less than 3 Å. As expected, all minimum values for atom−surface distance are larger, compared to those obtained for perpendicular orientation. The closest atoms to the surface are the hydrogens; the hydrogen−surface distances range from 2.22 Å (for dA) to 2.27 Å (for dG).

We compute the adsorption energy (or binding energy), ΔE_{ads}, for each nucleoside/Au composite. Here, we define ΔE_{ads} as the difference between the total energy of the composite and the sum of the total energies of the free relaxed molecule and the surface

$$\Delta E_{ads} = E_{dX/Au} - (E_{dX} + E_{Au}) \quad (1)$$

where X denotes A, T, G, and C. The respective adsorption energies are summarized in Table 1 (the BSSE corrections were taken into account). The negative values of ΔE_{ads} imply a stable adsorption for all eight composite systems. Overall, the parallel orientation is the most stable. In this case, the adsorption energies given in Table 1 follow the rule $\Delta E_{ads}^{dG} > \Delta E_{ads}^{dA} = \Delta E_{ads}^{dC} > \Delta E_{ads}^{dT}$, which is in qualitative agreement with the results of Mirkin et al.[18] For all systems, the ΔE_{ads} values are slightly larger than the value of 0.5 eV, which is generally accepted as the transition limit from the physisorption to chemisorption.

We note that for dA the adsorption energies are almost equal in the two configurations. On the other hand, for the dG adsorbed perpendicular with respect to the surface, ΔE_{ads} is −0.27 eV, indicating that only physisorption takes place, while dG has the strongest binding energy in the parallel configuration (ΔE_{ads} = −0.69 eV). This makes dG the most selective nucleoside with respect to the adsorption geometry.

We compute the total deformation energy of the adsorbed molecules defined as $\Delta E_d = E_{adsorbed} - E_{free}$; E_{free} is the total energy of the free, relaxed nucleoside, while $E_{adsorbed}$ is the total

dx.doi.org/10.1021/jp210229e | J. Phys. Chem. C 2012, 116, 7351−7359

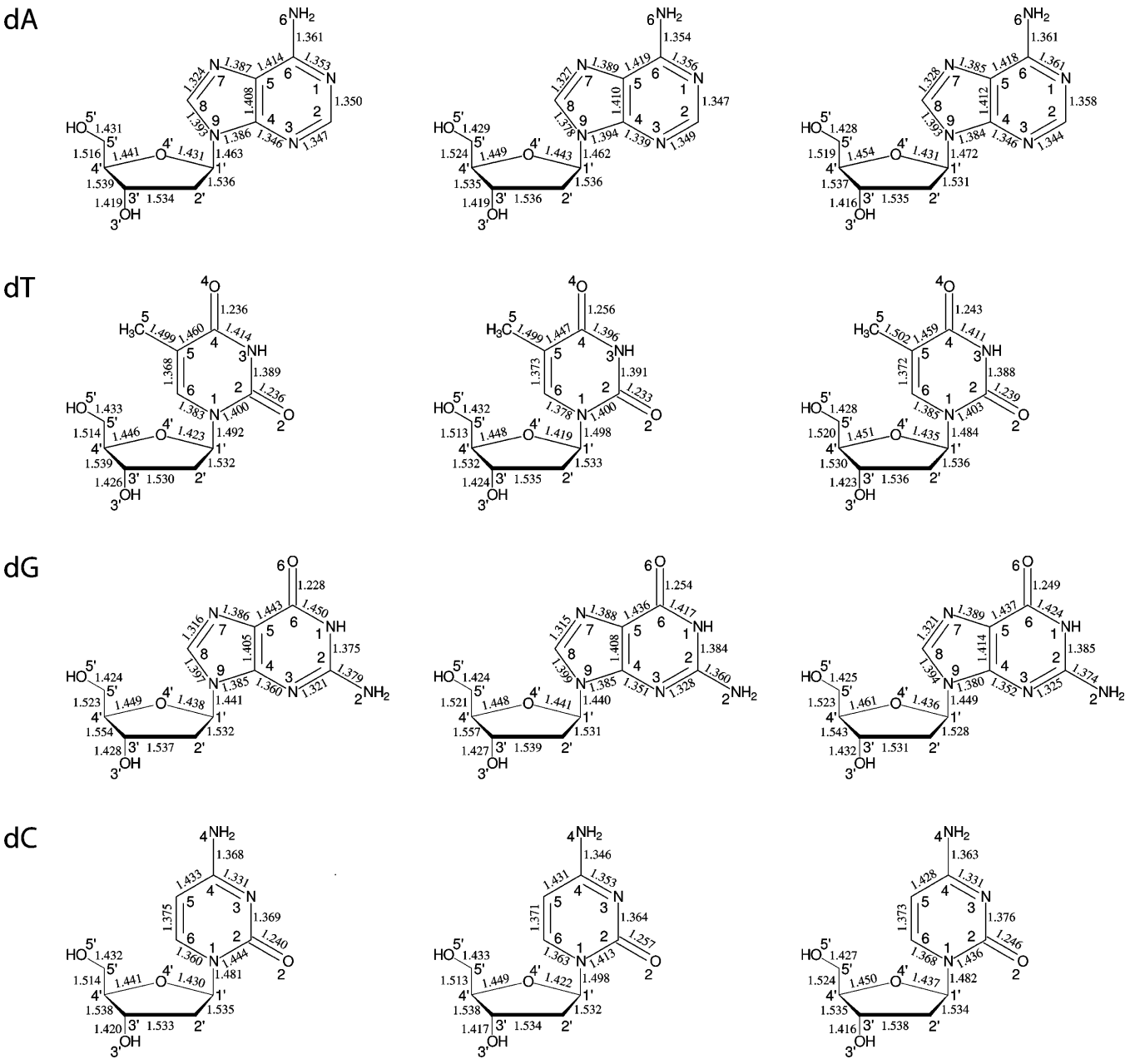

Figure 1. Calculated bond lengths for free nucleosides (left panel), adsorbed in perpendicular orientation (middle panel) and adsorbed in parallel orientation (right panel).

energy of the same nucleosides, but deformed by the adsorption on the surface. The values of ΔE_d for all configurations investigated in the present work are listed in Table 1. We note that ΔE_d values in the case of perpendicular orientation are typically small or negligible (in the case of dT). Parallel orientation leads to larger values of the ΔE_d; the exception to this rule is dG, where the deformation energy in the case of parallel orientation is smaller compared to the perpendicular one. Finally, the maximum value for ΔE_d occurs in the case of parallel orientations and reaches 0.2 eV for dC (i.e., almost 40% of the binding energy).

The computed bond lengths for the adsorbed and gas-phase molecules are compared in Figure 1. For the perpendicular orientation, we note that the C−NH_2 bond length presents a decreasing trend with respect to the values obtained in the gas phase (the shortening is 0.5% for dA, 1.6% for dC, and 1.4% for dG). For dC and dG, the reduction of the C−NH_2 bond occurs simmultaneously with an increase of the C−O bond length; the values are 1.4% for dC and 2.1% for dG. This can be explained by the reorganization of more positive charge on the NH_2 group and more negative charge on the oxygen atom, leading to changes in other double and single bonds in the aromatic ring, which compensate the total charge on the molecule. As a result, new resonance structures are formed in these two nucleosides. On the other hand, for dT, where no NH_2 group is present, the *C*4−*O*4′ bond length increases by 1.6%.

The variation of the bond lengths in the sugar moiety are smaller compared to those in the nucleobases. The values are typically in the range of computational errors (i.e., from 0.1 up to a maximum value of 0.6% for the *C*4′−*O*4′ bond length in dA and dC).

dx.doi.org/10.1021/jp210229e | *J. Phys. Chem. C* 2012, 116, 7351−7359

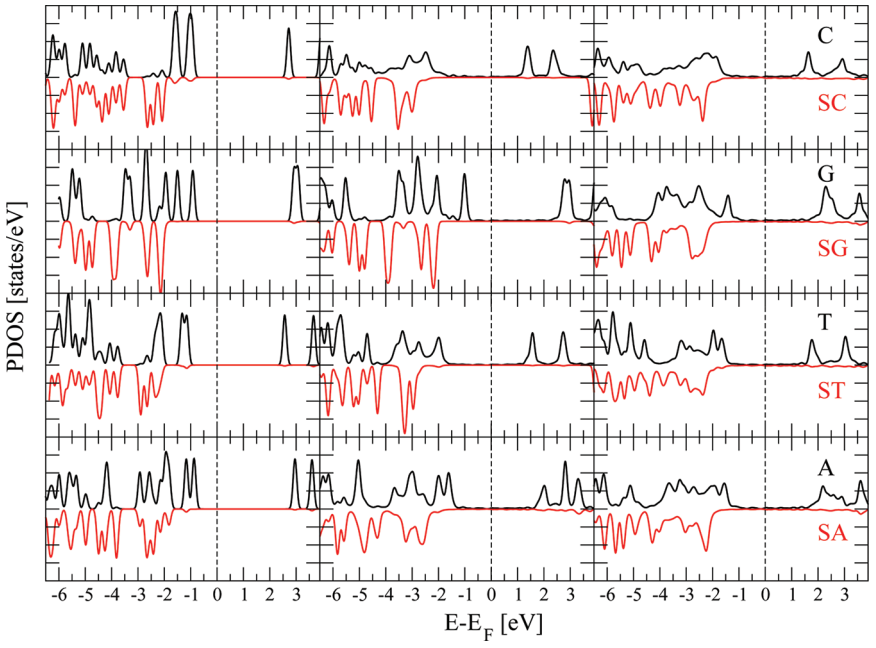

Figure 2. PDOS for nucleosides: free (left panel) and oriented perpendicular (middle) and parallel (right) with respect to the gold surface. Black curves, DNA bases projected density of states; red curves, the corresponding sugar moieties. The Fermi level of the molecule−metal systems was set to zero; for the free molecules we lined up the vacuum level of the clean surface (i.e., the average of the Hartree potential in vacuum) with the vacuum level of the free molecules.

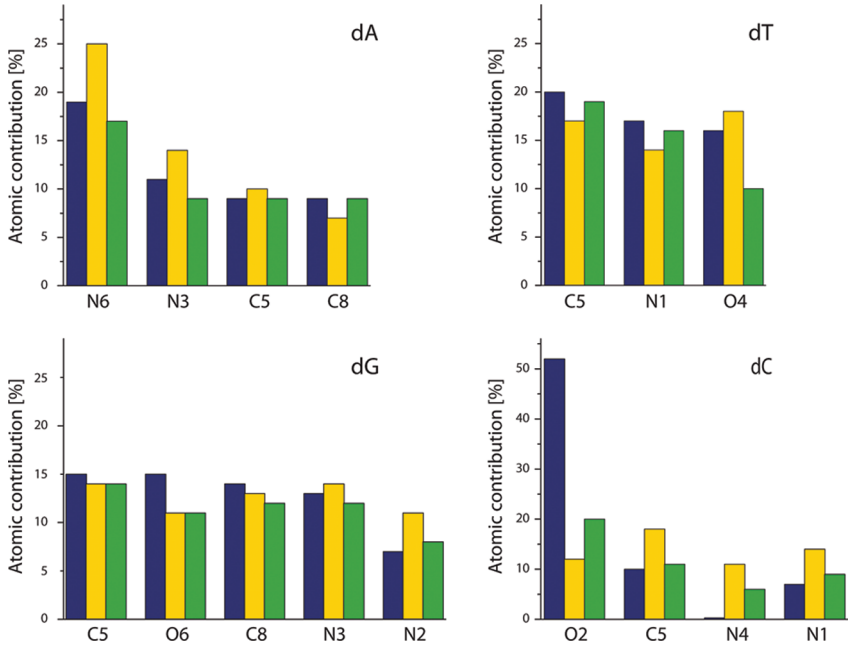

Figure 3. Atomic contribution to the HOMO orbital for DNA nucleosides: free (dark blue), adsorbed perpendicular (yellow), and adsorbed parallel (green) to the surface.

In the case of parallel adsorption geometry, we see that the trends for bond length variations are similar to those present at perpendicular orientation (i.e., decrease of C−NH_2 bond length and increase for C−O bond lengths in adsorbed dA, dC, and dG). Nevertheless, the changes in the bond lengths are typically close to the limit of the computational accuracy (i.e., about 0.5%).

In the sugar moiety of parallel adsorbed nucleosides, an increase of the *C4′−O4′* bond length is present. In this case, the values are slightly larger with respect to those obtained in the case of normal adsorption. This is not a surprise since, for the parallel orientation, a direct interaction between the sugar and gold surface occurs. The maximum increase in the bond length is 0.9% for dA (in the case of the *C4′−O4′* bond).

Density of States. We compute the density of states (DOS) projected over the molecular orbitals of bases and sugar moieties for free and adsorbed nucleosides; the results are given in Figure 2. Our electronic structure calculations confirm that all free nucleosides have a large HOMO−LUMO gap (≈4 eV) and pretty similar electronic structures in the energy range

dx.doi.org/10.1021/jp210229e | *J. Phys. Chem. C* 2012, 116, 7351−7359

around their HOMO−LUMO orbitals (see Figure 2, left panel). We note that the energy spacing between the two LUMOs of guanine is around 0.1 eV, which is much smaller than for other base molecules. In contrast, the HOMO of guanine is separated by 0.6 eV from other occupied levels, whereas the energy spacing between the HOMO and the HOMO−1 for the other bases is smaller. The contribution of the sugar moiety to the DOS peaks of free molecules is negligible for both HOMO and LUMO orbitals. Instead, a large contribution of the sugar occurs at lower energies (about 2 eV below HOMO).

Upon the adsorption, the HOMO of dA is shifted by about −0.5 eV (i.e., is stabilized), while its amplitude is reduced up to almost 50% for the parallel orientation. We also note that the gap between HOMO−1 and HOMO−2 orbitals vanishes for parallel adsorption geometry. In the case of dT, the shift of the HOMO orbital is about −0.9 eV for perpendicular orientation, while for the parallel one the value is −0.6 eV. Also, the amplitudes of the HOMO and HOMO−1 peaks are significantly reduced, compared to the corresponding values in the free molecule. Remarkably, for dG adsorbed in perpendicular orientation we notice small changes of the HOMO−LUMO orbitals upon the adsorption, which is consistent with the weak physisorption hypothesis. In particular, the HOMO orbital is not shifted for the perpendicular adsorption geometry. On the other hand, parallel orientation brings a downward shift (about −0.25 eV) of the guanine's HOMO and a diminution of its amplitude. The most spectacular changes in the electronic structure occur for adsorbed cytosine. For dC, in both orientations, the HOMO is shifted downward with about 1 eV, and its amplitude is reduced to a half. This is consistent with the relative large deformation energy for the dC adsorbed in both perpendicular (0.06 eV) and parallel configurations (0.2 eV).

To rationalize these results, let us recall the d-band model of the reactivity of metal surfaces.[45] According to it, the interaction between the HOMO molecular (localized) orbitals and metal d-bands can be described by a two-level model. This is a consequence of the narrow bandwidth of the metal d-orbitals, which can be assimilated with an energy level. As a consequence, a downshift of the energy of HOMO orbitals occurs (while LUMO is shifted upward). Nevertheless, we note that for all DNA bases the molecular HOMO−LUMO gap of the adsorbed molecules remains roughly unchanged with respect to that of the molecules in the gas-phase, indicating the weak chemical interaction between molecules and the surface.

We go now to a detailed investigation of the atomic contributions to the HOMO orbitals. In Figure 3, we present the most important atomic contribution to the HOMO orbitals of the four nucleosides in the gas-phase, as well as adsorbed on the gold surface. These contributions were extracted by comparing the value of the atomic-projected density of states at the energy of the HOMO orbitals. Contributions larger than 10% are displayed in Figure 3.

For dA, we note that the two atoms with dominant contributions to the HOMO (i.e., *N*6 and *N*3) have similar behavior upon the adsorption of the molecule in both orientations. Precisely, while for perpendicular orientation the *N*6 and *N*3 contribution to the HOMO orbital is increasing, for the parallel one this contribution is lowered. This corroborates with the 0.5% shortening of the *C*6−NH_2 bond discussed above. On the other hand, for parallel configuration the same analysis shows that the contribution of *N*3 to the HOMO is slightly smaller compared to the free molecule; accordingly, no change in the *C*6−NH_2 bond length is seen. For the other two atoms with relatively large contributions, we note weak modifications of their contribution to the HOMO orbital.

In the case of dT, we note that the influence of the surface upon the HOMO's structure is less important compared to that observed for dA. The important modification of the *C*4−O bond length is only qualitatively reflected in the HOMO structure; precisely, the *O*4 contribution for dT adsorbed in perpendicular configuration is only slightly increased, while the *C*4−O bond length variation in dT is one of the largest among the four nucleosides. The adsorption in the parallel orientation leads to a dramatic decrease of oxygen contribution to the HOMO orbital (about one-half, with respect to the corresponding value for the perpendicular oriented adsorption).

In the case of dG, we found the smallest influence of the adsorption geometry upon the HOMO of the molecule. For the *C*5 atom, the variations with respect to the gas phase are negligible. For *O*6 and *N*2 atoms, we found relatively important modifications with respect to the gas phase, indicating that the oxygen and NH_2 group interact with the gold surface. For both orientations, the contribution of *O*6 diminishes upon the adsorption, while that of *N*2 increases.

The most spectacular behavior occurs for the HOMO orbital of dC. On one hand, the *O*2 has a dominant contribution to the HOMO orbital of the free molecule (slightly more than 50%). This contribution is reduced to 13% for the perpendicular adsorption geometry and is about 20% for the parallel one. Also, we note that the *N*4 acquires a relative weight of 12% for perpendicular orientation, while its contribution to the HOMO of free dC is less than 1%. For parallel orientation, *N*4 still contributes with 7% to the PDOS of the HOMO. These are indications for the presence of chemical interaction between dC and the gold surface, with the *O*4 and NH_2 playing the dominant role.

Charge Transfer. The investigation of the molecule−metal interaction has to include the analysis of the charge redistribution in the molecular structure adsorbed on the metallic surface. Therefore, we analyze the spatially resolved charge-density difference

$$\Delta\rho(\vec{r}) = \rho_{ads/subs}(\vec{r}) - [\rho_{ads}(\vec{r}) + \rho_{subs}(\vec{r})] \quad (2)$$

where $\rho_{ads/subs}(\vec{r})$, $\rho_{ads}(\vec{r})$, and $\rho_{subs}(\vec{r})$ are the (negative) charge densities of the relaxed adsorbate−substrate system, adsorbate without substrate, and clean relaxed surface, respectively. The contour plot of $\Delta\rho(\vec{r})$ in the plane of DNA bases (i.e., the effects of electronic density fluctuations on σ bonds is taken into account) is given in Figure 4. In Figure 5 we represent the 3D contours for $\Delta\rho(\vec{r})$.

In the case of a perpendicular orientation, we notice from Figure 4 that the electronic density is depleted between the nucleoside and surface, for all cases. For dA, the depletion takes place between the *N*7 and the gold atom in the surface, while an increase of the electronic density occurs around the NH_2 group. For dT, the contour plots indicate that the decrease of electronic density has high values in the vicinity of the *O*4 atom. Note that the *O*4 sits in a hollow position with respect to the gold surface; therefore, the corresponding charge reorganization is only partially visible in Figure 4. In the case of dG, in addition to the loss of electrons in the region between *O*6 and the gold surface, a slight accumulation of electrons takes place

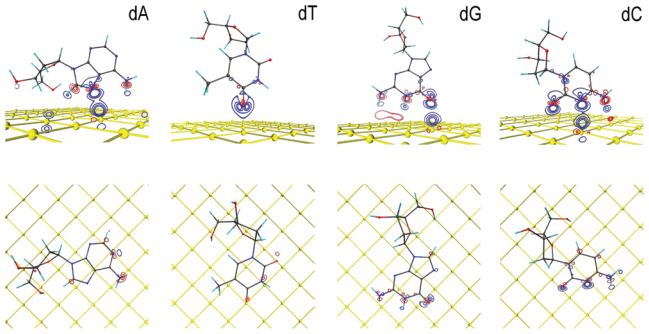

Figure 4. Contour plots of the $\Delta\rho(\vec{r})$ defined in eq 2 for the two adsorption geometries: perpendicular (top) and parallel (bottom). Contour increment: 0.003 e/Bohr^3. Only the upper layer of the gold surface is shown. We use red/blue colors for negative/positive contour values (i.e., electric charges).

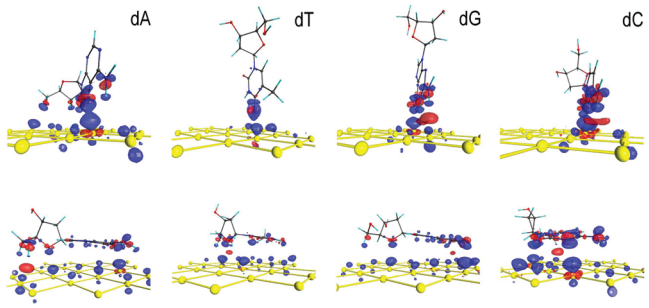

Figure 5. 3D representation of the $\Delta\rho(\vec{r})$ defined in eq 2 for the parallel adsorption geometry. We plot surfaces at constant value on the contour of 0.003 e/Bohr^3. Only the upper layer of the gold surface is shown. We use red/blue colors for negative/positive contour values (i.e., electric charges).

between the *N*1 and the surface. Finally, for dC, the electronic density is depleted in the region between *N*3 and its closest gold atom. Also, the same occurs in the vicinity of NH_2 and *O*2 atoms.

For the parallel orientation, the redistribution of charge in the plane of DNA bases is less important compared to that occurring for the perpendicular orientation. Interestingly, for dA and dT we see positive charge in the $\Delta\rho(\vec{r})$ contour plots, while for dC and dG a negative charge accumulation is dominant in the bases' plane.

Complementary information is brought by Figure 5, where a 3D equivalent of Figure 4 is presented. We see that, in the case of parallel orientation, important fluctuations of the charge density occur also, but they are spread over the whole π rings. This is consistent with previous findings, where smaller values on the contour plots of the $\Delta\rho(\vec{r})$ were put in evidence (see Figure 4). In particular, we see that for the parallel orientation the sugar moiety is also affected by the charge redistribution, unlike in the case of perpendicular orientation.

In Table 2, the Mülliken populations for the net charge on the molecules (free and adsorbed) are given. In the free molecules, a transfer of the electrons occurs between the base and sugar. For the free molecules, this transfer ranges between 0.21 (dT) to 0.09 (dG). Upon the adsorption of nucleosides on the gold surface, the Mülliken charges may vary by up to 60% (see, for example, the results for dC). Typically, a decrease of the Mülliken charge on all adsorbed DNA bases occurs. For the sugar moiety, the behavior is more complex; if the oxygen is present in the structure of the DNA bases (i.e., for T, G, and C), the Mülliken charges increase at perpendicular orientation and decrease at parallel geometry. In the case of dA oriented perpendicular with respect to the surface, this trend is not observed. Precisely, a decrease from −0.17 to −0.11 is present.

Table 2. Total Mülliken Charges for Nucleosides in Interaction with the Gold Surface for Perpendicular and Parallel Orientations[a]

	free	perpendicular	parallel
dA	0.17 (−0.17)	0.12 (−0.11)	0.12 (−0.06)
dT	0.21 (−0.21)	0.13 (−0.23)	0.16 (−0.06)
dG	0.09 (−0.09)	0.16 (−0.09)	0.09 (−0.08)
dC	0.18 (−0.18)	0.06 (−0.23)	0.06 (−0.08)

[a]Values in parentheses are for the sugar moiety.

The Mülliken charges are known to be basis-dependent quantities, and the errors in computing the charge transfer based on Mülliken populations are known to be significant. By comparing the Mülliken charges obtained by us for free nucleosides with Weinhold's natural population analysis (NPS) of Richardson et al.,[44] we found significant differences. While the results are qualitatively the same, the value of the charge transfer between sugar and base resulting from NPS is roughly equal in all cases (i.e., about 0.28 electrons are transferred from base to sugar). Mülliken charges predict a value of 0.09 for dG which is clearly underestimated.

Therefore, we supplement our charge transfer analysis by a detailed analysis of the $\Delta\rho(\vec{r})$ defined in eq 2. Precisely, we estimate the charge transfer by integrating $\Delta\rho(\vec{r})$ over selected spatial domains. Also, to assess the role of the electrostatic contribution to the molecule−surface bonding,[46−48] we use an approach similar to that proposed by Preuss et al.[46] to estimate the electrostatic interaction energy resulting from the molecule−surface charge transfer.

We divide the adstructure into two regions by a plane parallel to the metal's surface (we call them R_1 and R_2). The former one contains the ad-molecule, and the latter one contains the surface. The total electrostatic energy can be computed by making use of the geometrical separation of the space into two regions and of the $\Delta\rho(\vec{r})$, defined in eq 2.

This energy is given by the formula

$$E_{\mathrm{el}} = \frac{1}{4\pi\varepsilon_0} \sum_{i\in R_1, j\in R_2} \frac{Q_i Q_j}{r_{ij}} \qquad (3)$$

where the indices i and j run over the points located in region R_1 or R_2, respectively.[49] The charge corresponding to the grid point i is computed as $Q_i = \Delta\rho_i(\vec{r})\delta V)$, where $\Delta\rho_i(\vec{r})$ is the value of $\Delta\rho(\vec{r})$ stored at the point i on the grid and δV is the volume associated with a point on the grid. Finally, r_{ij} represents the physical distance between the two grid points, i and j. The numerical results obviously depend on the way the adsorbate system is divided into the two regions (the position of the separating plane). Nevertheless, the method allows us to give a quantitative estimation of the importance of the charge transfer interaction occurring between the molecule and surface. We define the two regions by choosing a plane parallel to the metal surface and located at 1 Å distance from it (i.e., close to the plane that bisects the ad-system at the vertical position). This choice is supported by the results presented in Figure 4 and Figure 5: a depletion of $\Delta\rho(\vec{r})$ is present close to this plane, which allows a separation of $\Delta\rho(\vec{r})$ in two spatial regions.

dx.doi.org/10.1021/jp210229e | J. Phys. Chem. C 2012, 116, 7351−7359

The results summarized in Table 3 show that the electrostatic energy is repulsive, but its effects upon the total binding energy are negligible for both orientations. Relatively important values occur for dC; nevertheless, the electrostatic energy represents here less than 10% of the total energy for perpendicular orientation and 5% for the parallel one. The electrostatic interaction is typically stronger for the perpendicular orientation. This is probably caused by the localization of $\Delta\rho$ in the region between the nucleoside's atoms and the gold surface (see also Figure 5). Furthermore, this localization is specific to the perpendicular orientation: the highly electronegative atoms (nitrogen and oxygen) are in close contact to the surface. In the case of parallel orientation, the interaction takes place between the surface and the π rings. This leads to a transfer of the electrons from the surface to the molecule: the HOMO orbitals of all nucleosides lie at about −1.5 eV below the Fermi level of the metal, and this favors the transfer of electrons from the surface to the molecule.

Table 3. Electrostatic Energy (ΔE_{el}) and Electronic Populations ($n_{molecule}$) for Nucleosides in Interaction with the Gold Surface for the Two Orientations

		dA/Au	dT/Au	dG/Au	dC/Au
perpendicular orientation	ΔE_{el} [eV]	0.03	0.00	0.02	0.04
	$n_{molecule}$	−0.03	−0.03	−0.01	−0.08
parallel orientation	ΔE_{el} [eV]	0.01	0.00	0.00	0.02
	$n_{molecule}$	0.05	0.05	0.04	0.02

The total electronic population on the molecule is negative for perpendicular orientation, while it became positive for parallel orientation. The electron loss in the molecule's region for perpendicular orientation ranges from 0.01 (dG) to a maximum of 0.08 (dC). At parallel orientation, the increase of electronic population has a minimum of 0.02 (dC), while the maximum value is 0.05 (dA). In the latter case, the transfer occurs between surface and the π rings, and the values of the total charge transfer are less dispersed compared to those obtained at perpendicular orientation.

As we already mentioned, the results listed in Table 3 depend on the position of the plane that separates the molecule-like region from the surface region, so this conclusion should be seen from a qualitative perspective. To strengthen this point, we performed additional investigations for dA oriented perpendicular to the surface by computing the total charge and interaction energy for different positions of the separation plane. For distances of the surface-separation plane ranging from 0.7 to 1.3 Å above the surface, we found values of the electronic population in the molecule region between −0.07 and −0.02. This result can be qualitatively understood if we inspect Figure 4: $\Delta\rho(\vec{r})$ is depleted in the region between the *N*7 atom and the Au surface, which makes the result of charge integration relatively stable with respect to the value set for the *Z*-coordinate of the separation plane. The same qualitative argument is valid for the other systems.

CONCLUSION

In this paper, we have numerically addressed specifics of adsorption of each DNA nucleoside on the (100) gold surface. The calculations are based on DFT with the PBE functional, a double-ζ LCAO basis set, and norm-conserving pseudopotentials.

We investigate two adsorption geometries, perpendicular and parallel with respect to the surface, and we find that all nucleosides are adsorbed with their corresponding DNA bases almost parallel to the Au(100) surface. Perpendicular orientation is also possible for all nucleosides, but the bond energy is lowered by this configuration. The only exception is adenosine: in this case the binding energies in the two configurations are almost equal, while for guanosine the binding energy is strongly dependent on the relative orientation of the guanine and Au surface.

Our analysis reveals a qualitative dependence of the molecule−surface charge transfer in the two orientations. Precisely, for all nucleosides adsorbed at perpendicular orientation, the total electronic population decreases upon adsorption, as a consequence of the interaction between gold and specific groups of highly electronegative atoms (like NH_2 and oxygen). For the parallel orientation, the main molecule−surface interaction takes place between the metal and the π rings; the electronic population of adsorbed nucleosides increases.

The dominant molecule−metal interaction mechanism is the strong physisorption with adsorption energies of −0.53 eV (dA), −0.52 eV (dT), −0.69 eV (dG), and −0.53 eV (dC), respectively. The analysis of the atomic contributions to the HOMO orbitals of the DNA nucleosides shows that only weak chemical interaction between molecules and surface occurs. Our calculations demonstrate that the influence of the metallic surface on the electronic orbitals of adsorbed nucleosides is the strongest for the dC. Precisely, the important contribution of the oxygen atom to the HOMO of the gas-phase molecule is suppressed when dC is adsorbed on the gold surface. On the contrary, the nitrogen atom in the NH_2 group has contributions to the HOMO of the adsorbed molecule, unlike in the gas-phase.

Understanding the details of bond formation between nucleic acids and noble metal surfaces asks for thorough investigation of the physical properties of the adsorbate systems at the molecular level. We extract information by corroborating the geometric properties of the adsorbate, the density of states, and the nucleoside−surface charge transfer. This approach allows us to draw a picture of the adsorption mechanism occurring for each nucleoside and points out similarities and differences between the electronic structure of adsorbed nucleosides.

AUTHOR INFORMATION

Corresponding Author

*E-mail: cristian.morari@itim-cj.ro. Phone: +40 264 584037. Fax: +40 264 420042.

Notes

The authors declare no competing financial interest.

ACKNOWLEDGMENTS

We thank Dr. Ioana Grosu for helpful discussions. We acknowledge financial support from the Core Program, project PN 09-440101, contract no. 44N/2009. Thanks are due to NIRDIMT Cluj-Napoca Data Center for providing computer facilities.

REFERENCES

(1) Waser, R., Ed. *Nanoelectronics and Information Technology*; Wiley: Weinheim, 2003.

(2) Balzani, V.; Credi, A.; Venturi, M., Eds.; *Molecular Devices and Machines - A Journey into the Nanoworld*; Wiley: Weinheim, 2003.

(3) Feringa, B. L. *Molecular Switches*; Wiley: Weinheim, 2001.
(4) Bryce, M. R.; Petty, M. C.; Bloor, D. *Molecular Electronics*; Oxford University Press: New York, 1995.
(5) Cuniberti, G.; Fagas, F.; Richter, K., Eds.; *Introducing Molecular Electronics*; Springer: Berlin, Heidelberg, 2005.
(6) Tao, N. J.; de Rose, J. A.; Lindsay, S. M. *J. Phys. Chem.* **1993**, *97*, 910−919.
(7) Mirkin, C. A.; Letsinger, R. L.; Mucic, R. C.; Storhoff, J. J. *Nature* **1996**, *382*, 607−609.
(8) Alivisatos, A. P.; Johnsson, K. P.; Peng, X.; Wislon, T. E.; Loweth, C. J.; Bruchez, M. P. Jr.; Schultz, G. C. *Nature* **1996**, *382*, 609−611.
(9) Storhoff, J. J.; Lazarides, A. A.; Mucic, R. C.; Mirkin, C. A.; Letsinger, R. L.; Schatz, G. C. *J. Am. Chem. Soc.* **2000**, *122*, 4640−4650.
(10) Park, S.-J.; Lazarides, A. A.; Mirkin, C. A.; Letsinger, R. L. *Angew. Chem., Int. Ed.* **2001**, *40*, 2909−2912.
(11) Niemeyer, C. M. *Angew. Chem., Int. Ed.* **2001**, *40*, 4129−4158.
(12) Harnack, O.; Ford, W. E.; Yasuda, A.; Wessels, J. M. *Nano Lett.* **2002**, *2*, 919−923.
(13) Parak, W. J.; Pellegrino, T.; Micheel, C. M.; Gerion, D.; Williams, S. C.; Alivisatos, A. P. *Nano Lett.* **2003**, *3*, 33−36.
(14) Remacle, F.; Kryachko, E. S. *Nano Lett.* **2005**, *5*, 735−739.
(15) Remacle, F.; Kryachko, E. S. *J. Phys. Chem. B* **2005**, *109*, 22746−22757.
(16) Kryachko, E. S. *J. Mol. Struct.* **2008**, *880*, 23−30.
(17) Kimura-Suda, H.; Petrovykh, D. Y.; Tarlov, M. J.; Whitman, L. J. *J. Am. Chem. Soc.* **2003**, *125*, 9014−9015.
(18) Demers, L.; Östblom, M.; Zhang, H.; Jang, N.-H.; Liedberg, B.; Mirkin, C. A. *J. Am. Chem. Soc.* **2002**, *124*, 11248−11249.
(19) Chen, Q.; Frankel, D. J.; Richardson, N. V. *Langmuir* **2002**, *18*, 3219−3225.
(20) Giese, B.; McNaughton, D. *J. Phys. Chem. B* **2002**, *106*, 101−112.
(21) Li, W.; Haiss, W.; Floate, S.; Nichols, R. *Langmuir* **1999**, *15*, 4875−4883.
(22) Roelfs, B.; Baumgärtel, H. *Ber. Bunsen-Ges. Phys. Chem.* **1995**, *99*, 677−681.
(23) Kim, S. K.; Joo, T. H.; Suh, S. W.; Kim, M. S. *J. Raman Spectrosc.* **1986**, *17*, 381−386.
(24) Koglin, E.; Sequaris, J. M.; Valenta, P. *J. Mol. Struct.* **1980**, *60*, 421−425.
(25) Suh, J. S.; Moskovits, M. *J. Am. Chem. Soc.* **1986**, *108*, 4711−4718.
(26) Badr, Y.; Mahmoud, M. A. *Spectrochim. Acta A* **2006**, *63*, 639−645.
(27) Piana, S.; Bilic, A. *J. Phys. Chem. B* **2006**, *110*, 23467−23471.
(28) Watanabe, T.; Kawanami, O.; Katoh, H.; Honda, K.; Nishimura, Y; Tsuboi, M. *Surf. Sci.* **1985**, *158*, 341−351.
(29) Otto, C.; Van den Tweel, T. J. J.; de Mul, F. F. M.; Greve, J. *J. Raman Spectrosc.* **1986**, *17*, 289−298.
(30) McNutt, A.; Haq, S.; Raval, R. *Surf. Sci.* **2003**, *531*, 131−144.
(31) Rauls, E.; Blankenburg, S.; Schmidt, W. G. *Surf. Sci.* **2008**, *602*, 2170−2174.
(32) Plekan, O.; Feyer, V.; Ptasińska, S.; Tsud, N.; Cháb, V.; Matolín, V.; Prince, K. C. *J. Phys. Chem. C* **2010**, *114*, 15036−15041.
(33) Feyer, V.; Plekan, O.; Prince, K. C.; Šutara, F.; Skála, T.; Cháb, V.; Matolín, V.; Stenuit, G.; Umari, P. *Phys. Rev. B* **2009**, *79*, 155432.
(34) Yang, B.; Wang, Y.; Li, G.; Cun, H.; Ma, Y.; Du, S.; Xu, M.; Song, Y.; Gao, H.-J. *J. Phys. Chem. C* **2009**, *113*, 17590−17594.
(35) Jang, N. H. *Bull. Korean Chem. Soc.* **2002**, *23*, 1790−1800.
(36) Pergolese, B.; Bonifacio, A.; Bigotto, A. *Phys. Chem. Chem. Phys.* **2005**, *7*, 3610−3613.
(37) Puzdder, A.; Williamson, A. J.; Zaitseva, N.; Galli, G.; Manna, L.; Alivisatos, A. P. *Nano Lett.* **2004**, *4*, 2361−2365.
(38) Barnard, A. S.; Curtiss, L. A. *Nano Lett.* **2005**, *5*, 1261−1266.
(39) Soler, J. M.; Artacho, E.; Gale, J. D.; García, A.; Junquera, J.; Ordejón, P.; Sanchez-Portal, D. *J. Phys.: Condens. Matter* **2002**, *14*, 2745−2779.
(40) Ordejón, P.; Artacho, E.; Soler, J. M. *Phys. Rev. B* **1996**, *53*, R10441.
(41) Perdew, J. P.; Burke, K.; Ernzerhof, M. *Phys. Rev. Lett.* **1996**, *77*, 3865−3868.
(42) Anglada, E.; Soler, J. M.; Junquera, J.; Artacho, E. *Phys. Rev. B* **2002**, *65*, 205101.
(43) Troullier, N.; Martins, J. L. *Phys. Rev. B* **1992**, *46*, 1754−1765.
(44) Richardson, N. A.; Gu, J; Wang, S; Xie, Y; Schaefer, H. F. III *J. Am. Chem. Soc.* **2004**, *126*, 4404−4411.
(45) Hammer, B.; Nørskov, J. K. *Surf. Sci.* **1995**, *343*, 211−220.
(46) Preuss, M.; Schmidt, W. G.; Bechstedt, F. *Phys. Rev. Lett.* **2005**, *94*, 236102.
(47) Hauschild, A.; Karki, K.; Cowie, B. C. C.; Rohlfing, M.; Tautz, F. S.; Sokolowski, M. *Phys. Rev. Lett.* **2005**, *94*, 036106.
(48) Alkauskas, A.; Baratoff, A.; Bruder, C. *Phys. Rev. B* **2006**, *73*, 165408.
(49) The full algorithm for the calculation of the electrostatic interaction includes a shift of the charge density within the supercell used for calculations to avoid the interactions between periodic images of the molecule.